Available online at www.sciencedirect.com

ScienceDirect

Solar Energy 103 (2014) 96–107

SOLAR ENERGY

www.elsevier.com/locate/solener

Discrete *I–V* model for partially shaded PV-arrays

Eloy Díaz-Dorado, José Cidrás, Camilo Carrillo *

University of Vigo, Spain

Received 19 November 2012; received in revised form 24 September 2013; accepted 29 January 2014

Communicated by: Associate Editor Hari Mohan Upadhyaya

Abstract

Photovoltaic systems that are partially shaded show changes in their *I–V* curve that makes its shape is different from that typically shown in unshaded PV panels. The effects of shading depend on several factors like electrical connections between elements or the geometry of the PV-cells.

This paper presents a generalized, quick and simple method for modelling and simulating the electrical behaviour of PV installations under any shading situation which is mainly based in the Bishop modelling. So, the proposed method models PV-systems by discretizing currents and voltages in PV-cells which are connected in series and parallel associations (PV-cells, PV-groups, PV-modules, PV-strings and PV-array). For the PV-cell, a non-linear and implicit function which takes into account forward and reverse biasing is considered. Bypass diodes have also been included in the model. The relationship between discrete currents and voltages is established using the Newton–Raphson algorithm, analytical approximations and interpolation methods.

The proposed method is used to provide a complete analysis of current, voltage and power in several PV systems under partial shading conditions.

Keywords: Photovoltaic systems; Photovoltaic cells; Partial shading

1. Introduction

The shading of a photovoltaic (PV) installation implies that may have PV-cells working in different irradiance conditions within the same installation. Thus, elements (cells or diodes) that are normally working forward (or reverse) biased could change its polarization. Furthermore, other working parameters (e.g. the PV-cell temperature) could be different between neighbouring elements. As a consequence, for a detailed analysis of the electrical behaviour of partially shaded PV installations, it is necessary take into account their simplest elements, cells and diodes, and the different parallel and series associations between them. The system of equations derived from this analysis is characterized by its large dimension and by being formed by non-linear equations. This system of equations usually presents convergence problems due to their strong nonlinearity.

Some authors propose several methods to study the PV systems based on Newton–Raphson (Karatepe et al., 2006; Quaschning and Hanitsch, 1996; Kawamura et al., 2003), Gauss–Seidel (Chatterjee et al., 2011), Lambert W-function and Newton–Raphson (Petrone and Ramos-Paja, 2011; Petrone et al., 2007) and piecewise-linear technique (Wang and Hsu, 2011).

Most authors have studied the behaviour of partial shading on individual photovoltaic modules (Quaschning and Hanitsch, 1996; Kawamura et al., 2003; Bishop, 1988; Caluianu et al., 2009; Alonso-García et al., 2006a;

* Corresponding author. Tel.: +34 986813912; fax: +34 986812173.
E-mail addresses: ediaz@uvigo.es (E. Díaz-Dorado), jcidras@uvigo.es (J. Cidrás), carrillo@uvigo.es (C. Carrillo).

http://dx.doi.org/10.1016/j.solener.2014.01.037
0038-092X/

Silvestre and Chouder, 2008; Chen and et al., 2010; Silvestre et al., 2009). Other authors have analyzed PV systems with various modules (Karatepe et al., 2006; Petrone and Ramos-Paja, 2011; Petrone et al., 2007; Bishop, 1988; Silvestre et al., 2009; Díaz-Dorado et al., 2010a, 2010b) but their results cannot generalized to model a PV array. Previous papers analyse the behaviour of modules or installations considering the actuation of the bypass diodes. However, only some authors have considered the behaviour of cells in reverse bias caused by shading and its effect on the generation (Quaschning and Hanitsch, 1996; Bishop, 1988; Silvestre et al., 2009; Alonso-García and Ruíz, 2006; García et al., 2008). In Bishop (1988), three types of interconnection circuits of PV-cells are considered including bypass diodes and blocking diodes.

In other cases, approximated values or limit values are considered to analyse the power losses of photovoltaic systems (Díaz-Dorado et al., 2010b, 2011; Alonso-García et al., 2006b; Narvarte and Lorenzo, 2008; Gordon and Wenger, 1991; Woyte et al., 2003; Martínez-Moreno et al., 2010; Di Piazza and Vitale, 2010; Perpiñán, 2012).

As an alternative method to avoid trying to solve large systems of non-linear equations, this paper presents a discrete method for modelling the *I–V* characteristics of PV-arrays under any shading condition. The proposed discrete method is an improvement, generalization and systematization of that introduced by Bishop (1988). The proposed one considers the Newton–Raphson algorithm to solve the implicit non-linear equations related to PV-cells, unlike the Bishop method that uses a two-step iterative process.

This allows to define the *I–V* characteristic of each PV-cell by means of discretized model. Consequently, a generic PV-array can be solved taking into account the electrical characteristics of series and parallel associations by using discretized models.

As a result, the proposed method overcomes the needing of solving a large system of non-linear equations (Karatepe et al., 2006). So, the typical problems of convergence and large time-consuming computations are overcame. Furthermore, this method does not require to do approximations to represent diodes and PV-cells, e.g. null voltage during forward biasing of diodes. It must be taken into account that the accuracy of the results only depends on the discretization step used for current and voltage variables.

This paper is organized into five sections. Section 2 presents the equations of the PV-cell, bypass diode and shading modelling. In Section 3, the proposed discrete model is developed, starting from the discretization of series associations (PV-cells, PV group, PV-module and PV-string) to the parallel association (PV-array). Section 4 analyses the behaviour of three PV installations with different partial shading conditions. Finally, the conclusions are presented in Section 5.

2. Modelling of PV-cells and shadows

A PV-array can be considered as a set of PV-cells and diodes with different series and parallel associations (Fig. 1). In general, a PV-array can be defined as a set of $NxRxMxL$ of PV-cells connected as follows: N PV-cells in series with a bypass diode form a PV-group, R PV-groups in series form a PV-module, M PV-modules in series form a PV-string and L PV-strings in parallel form the PV-array. From a mathematical point of view, a PV-array is an electrical network with two types of non-linear elements connected in series and/or parallel: PV-cells and bypass diodes.

The following paragraphs discuss the PV-cell model, the equation of the bypass diode and a proposed model for partial shading on a PV-array.

2.1. Modelling of PV-cell and bypass diode

Generally a PV-cell can be expressed by means of a non-linear relationship between four variables: current (I in A), voltage (V in V), irradiance (G in W/m^2) and cell temperature (T in K). In this paper, a non-linear implicit function is used for PV-cell, where T and G are supposed to be known, and V and I are the variables of the *I–V* model. The PV-cell is modelled using the following equation that allows the analysis of forward and reverse biasing (Bishop, 1988):

$$I = I_L - I_0\left(e^{\frac{qV+IR_s}{nk_BT}} - 1\right) - \frac{V+IR_s}{R_p}\left(1 + \frac{\alpha}{(1-\frac{V+IR_s}{V_{br}})^m}\right) \quad (1)$$

$$I_L = \frac{G}{G_0} I_{L0}$$

where G_0 is the irradiance under Standard Test Conditions (STC), k_B is Boltzmann constant, R_p is the cell shunt resistance, R_s the cell series resistance, V_{br} is the junction breakdown voltage, α is the fraction of ohmic current involved in avalanche breakdown, m is the avalanche breakdown exponent and q is the electron charge.

For the sake of simplicity, the temperature has been supposed to be constant in the PV-array. As a consequence, this equation in its implicit form can be written as:

$$f(V, I, G) = 0 \quad (2)$$

In Appendix A, experimental PV-cell curves and the parameters for this equation are shown.

Finally, for the bypass diode used in PV-group clusters, which are typically standard silicon rectifier diodes, the following equation can be used:

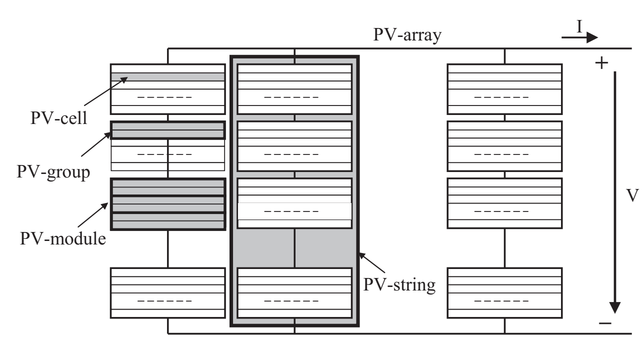

Fig. 1. Elements of a PV array.

$$I = I_0\left(e^{\frac{qV}{k_BT}} - 1\right) \quad (3)$$

where V and I are the voltage and current in the diode and I_0 is the reverse saturation current.

2.2. Modelling of partial shading on a PV-array

A PV-cell has two working regions: the forward bias region (PV-cell voltage: $V > 0$), where energy is generated, and the reverse bias region (PV-cell voltage: $V < 0$), where energy is consumed. In Appendix A, they are shown I–V curves of different PV-cells where forward bias and reverse bias have been considered (see Fig. 26).

Partial shading provoke a nonuniform irradiance distribution over the PV-array, as a consequence, each PV-cell in the array could have a different irradiance. In this paper, the shading has been represented by means of a model that relates the shading geometry with the irradiance. So, assuming the global irradiance G is composed by beam or direct irradiance G_b and diffuse irradiance G_d:

$$G = G_b + G_d \quad (4)$$

Then the shading effect over the "i" PV-cell can be expressed by:

$$G_i = \sigma_i \cdot G_b + G_d \quad (5)$$

where the parameter σ_i is noted as the shading coefficient. For a partially shaded cell the coefficient σ_i is:

$$\sigma_i = 1 - \zeta_i / A \quad (6)$$

where A is the area of the PV-cell and ζ_i is the shaded area, so σ_i is equal to 0 for a shaded cell and it is equal to 1 for a unshaded cell.

The complete simulation of a shaded array requires two types of data: (1) the electrical connection between PV-cells, PV-groups, PV-modules and PV-strings, in this way any PV-cluster can be electrically modelled, and (2) the geometric disposition of PV-cells in the array to allow the calculation of the effect of partial shading on each PV-cell (see Fig. 2).

3. Proposed method to obtain discrete *I–V* characteristics

According to the scheme of PV-array (see Fig. 1) and the shading conditions (see Fig. 2), in this paper, it is proposed a discrete method to systematically obtain the I–V characteristic of the PV-array as a whole. This discrete method starts with the analysis of PV-cells series association (see N-PV-cells in Fig. 4). Following the discretization of PV-group considering the bypass diode, the modelling of PV-module and PV-string are carried out. Finally, the PV-array is analyzed considering that is formed by a parallel association of PV-strings.

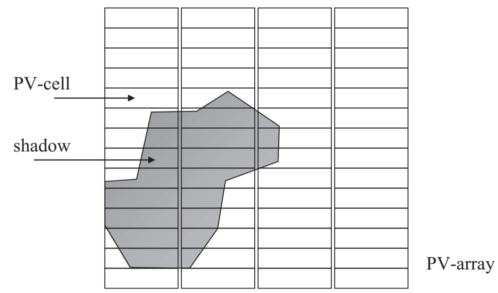

Fig. 2. Example of a shaded PV-array.

Therefore, the proposed discrete method takes into account two types of electrical associations (see Fig. 3) and, consequently, two basic processes: (i) series association, when PV-cells are in series and (ii) parallel association, when a set of PV-cells in series association has other elements in parallel.

In a series association, for a given current I the corresponding voltage for the element "i" can be obtained by means of the relation:

$$I \rightarrow f(V, I, G_i) \rightarrow V_i \quad (7)$$

where the existence of a unique solution derives from the fact that the function f is monotonically increasing (or decreasing). This can be applied for PV-cell and diode functions.

The resulting voltage of the complete association can be obtained by:

$$V = \sum_i V_i \quad (8)$$

Any solution for the series association can be expressed by means a (I, V_i) pair, taking into account that I is common to all the elements that form the series. So, the space of solutions might be represented by means of the current discrete vector $[I(k)]$ and its corresponding voltage

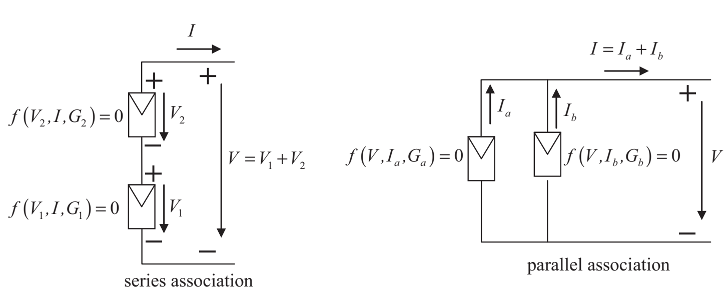

Fig. 3. Different types of element associations.

discrete vectors $[V(k)]_i$ and $[V(k)]$. For example, for two elements in series and a given current discrete vector, the voltage discrete vectors of each element can be obtained by:

$$I(k) \rightarrow \left\{ \begin{matrix} f(V, I(k), G_1) \rightarrow V_1(k) \\ f(V, I(k), G_2) \rightarrow V_2(k) \end{matrix} \right\} \rightarrow V(k) = V_1(k) + V_2(k) \tag{9}$$

For a parallel association, a similar procedure can be applied considering a set of common voltages $[V(k)]$ (see Fig. 3) by using the relation:

$$[V(k)] \rightarrow f(V, I, G_i) \rightarrow [I(k)]_i \tag{10}$$

3.1. N-PV-cells model

The N-PV-cells is a set of N PV-cells in series. The N-PV-cells cluster can be analyzed by means of a non-linear equation system of N equations, where the current I is common to all N cells:

$$[f(V_i, I, G_i)] = [0] \tag{11}$$

The minimum value considered for current I in PV-cells is zero when blocking diodes are installed in PV-strings, which is a common practice. The maximum value considered (I_{max}) is equal to the short-circuit current for the maximum irradiance. Using these extreme values the following discrete current vector is defined:

$$[I(k)] = [0, \Delta I, 2 \cdot \Delta I, \ldots, k \cdot \Delta I, \ldots, I_{\max}] \tag{12}$$

where

- ΔI is the discretization step for currents (see Appendix C);
- k is a positive integer number between $k = [1, \ldots, K]$ being K defined by $(K - 1) \cdot \Delta I = I_{\max}$. So each element of discrete vector is: $I_{(k)} = (k - 1) \cdot \Delta I$.

For each $I_{(k)}$ current, the voltage V_i in the i PV-cell can be obtained from (2) by Newton–Raphson using:

$$V_i^{(a)} = V_i^{(a-1)} + \frac{-f\left(V_i^{(a-1)}, I_{(k)}, G_i\right)}{\frac{\partial f\left(V_i^{(a-1)}, I_{(k)}, G_i\right)}{\partial V_i}} \tag{13}$$

where a is the number of iteration. Thus, N voltages V_i are obtained for each $I_{(k)}$ current (one for each i PV-cell) and, therefore, the voltage of N-PV-cells is expressed as:

$$V(k) = \sum_{i=1}^{N} V_i(k) \tag{14}$$

In conclusion, the N-PV-cells discrete model can be defined by the discrete vectors:

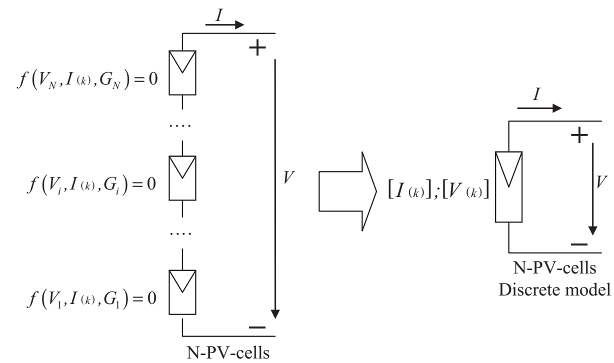

Fig. 4. Equivalent circuit of N-PV-cells.

$$\begin{aligned} [I_{(k)}] &= [I_{(1)}, I_{(2)}, I_{(3)}, \ldots, I_{(k)}, \ldots, I_{(K)}] \\ [V_{(k)}] &= [V_{(1)}, V_{(2)}, V_{(3)}, \ldots, V_{(k)}, \ldots, V_{(K)}] = \sum_{i=1}^{N} [V_{(k)}]_i \end{aligned} \tag{15}$$

In Fig. 4 is shown the N-PV-cells circuit and the discrete model of the N-PV-cells.

As an example, Fig. 5 presents the I–V curves of a system of 42-PV-cells, 33 of them with 1000 W/m^2 (unshaded) and 9 with 100 W/m^2 (shaded). The voltages for a current $I = 1.5$ A, also shown in the figure, are calculated by means of:

$$V = \sum_{i=1}^{42} V_i = 33 \cdot V_d + 9 \cdot V_h = 15.6 - 19.06 = -3.456 \text{ V}$$

where V_d is the voltage for unshaded PV-cells and V_h is the voltage for shaded PV-cells. They were obtained using the N–R method using (13).

3.2. PV-group model

A PV-group is composed by N-PV-cells and one bypass diode in parallel (see Fig. 6). The PV-group can be modelled by a non-linear system defined by:

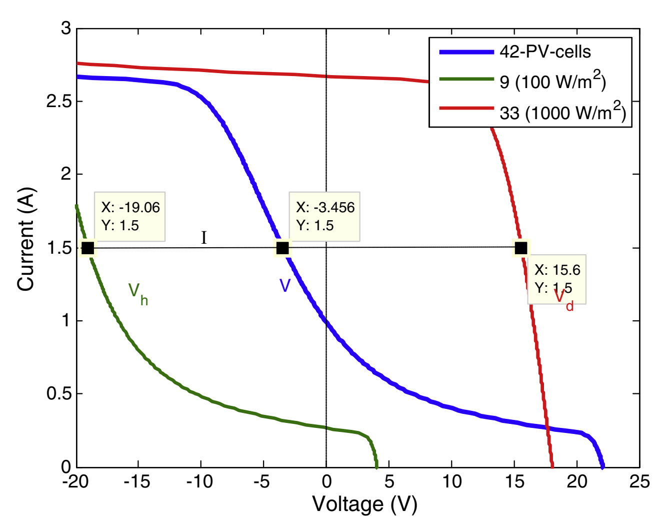

Fig. 5. I–V curves of 42-PV-cells: 33 unshaded and 9 shaded.

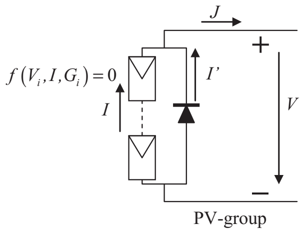

Fig. 6. Equivalent circuit of a PV-group.

$$\begin{cases} [f(V_i, I, G_i)] = [0] & \text{N-PV-cells in series} \\ I' = I_0\left(e^{\frac{-q\cdot V}{k_B T}} - 1\right) & \text{Bypass diode in parallel} \\ V = \sum_{i=1}^{N} V_i & \\ J = I + I' & \end{cases} \tag{16}$$

where

- I is the current in series cells;
- I' is the current in bypass diode;
- J is the output current of PV-group;
- V is PV-group voltage and V_i is the "i" PV-cell voltage.

The behaviour of the PV-group depends on the biasing of the bypass diode. When the diode is reverse biased the current through it is almost equal to zero, and the behaviour of the PV-group is the same as the behaviour of the N-PV-cells. On the other hand, when the diode is forward biased, the voltage of the PV-group depends on the current in the diode and in the N-PV-cells. As a consequence, the following procedure is used to obtain the current in the PV-group:

(1) The voltage and current pairs for PV-group can be represented by:

$$\begin{aligned} \left[J_{(k)}\right] &= \left[J_{(1)}, \ldots, J_{(K)}\right] \\ \left[V'_{(k)}\right] &= \left[V'_{(1)}, \ldots, V'_{(K)}\right] \end{aligned} \tag{17}$$

where must be taken into account that the set of values of current in vector $[J_{(k)}]$ are the same than those chosen for $\left[I_{(k)}\right]$, so:

$$\left[J_{(k)}\right] = \left[I_{(1)}, \ldots, I_{(K)}\right] \tag{18}$$

(2) For the voltage $V > 0$, the bypass diode presents reverse biasing, therefore, by (16) the bypass diode current is $I' \approx 0$. So, the discrete voltage vector can be written as:

$$\left[V'_{(k)}\right] = \left[V_{(1)}, V_{(2)}, \ldots, V_{(k)}, \ldots, V_{(K')}, V'_{(K'+1)}, \ldots, V'_{(K)}\right] \tag{19}$$

where K' represents the index of vector $[V_{(\mathrm{k})}]$ for N-PV-cells, defined in (15), when $V_{(\mathrm{K}')} \geqslant 0$ and $V_{(\mathrm{K}'+1)} < 0$. So the first K' elements of $[V'_{(k)}]$ are equal to those obtained for N-PV-cells.

(3) The diode is in forward biased when voltage V in N-PV-cells is negative. The transition between reverse and forward bias of the diode is defined by the current $I_{V=0}$ at zero voltage ($V = 0$) and it can be obtained from:

$$I_{V=0} = I_{(K')} + \frac{\Delta I}{V_{(K'+1)} - V_{(K')}} \cdot (0 - V_{(K')}) \tag{20}$$

Nevertheless, if the ΔI step is small enough, it can be assumed that $V_{(K')} \approx 0$ and $I_{V=0} \approx I_{(K')}$.

(4) For the voltage $V < 0$ the bypass diode presents forward biasing, therefore, using (16), the PV-group voltage is limited by the bypass diode. To obtain the resulting voltages, an incremental equivalent circuit for voltage $V < 0$ can be used (see Appendix B) and the following results can be derived:

$$\begin{cases} I \approx I_{V=0} \\ J = I' + I_{V=0} \end{cases} \tag{21}$$

So, according to (3), (20) and (21), elements from $K' + 1$ to K of $[V'_{(k)}]$ can be obtained using:

$$V'_{(k)} = -\frac{k_B T}{q} \cdot Ln\left(\frac{I_{(k)} - I_{V=0}}{I_0} + 1\right) \tag{22}$$

The equivalent circuit and the discrete model of a PV-group are shown in Fig. 7.

As an example, Fig. 8 presents the I–V curve of a PV-group constituted by 42-PV-cells: 33 with 1000 W/m^2 (unshaded) and 9 with 100 W/m^2 (shaded) and a bypass diode. This case is the same as shown in Fig. 5 but including the bypass diode.

3.3. PV-module model

A PV-module is a series association of the R PV-groups. Therefore, the discrete model of the PV-module is the result of the association of the R PV-groups with the same current $J_{(k)}$. So, the R PV-groups can be defined by vectors:

$$[J_{(k)}];\left[V'_{(k)}\right]_{r=1,\ldots,R} \tag{23}$$

In this way, the discrete model of the PV-module (see equivalent circuit of Fig. 9) is defined by the discrete vectors:

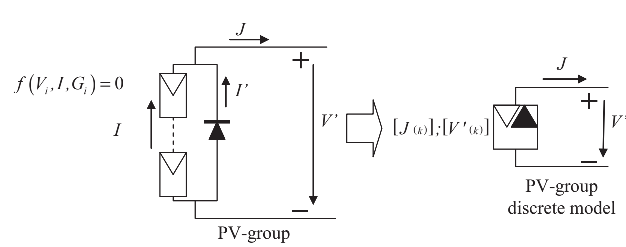

Fig. 7. Equivalent circuit and discrete model of a PV-group.

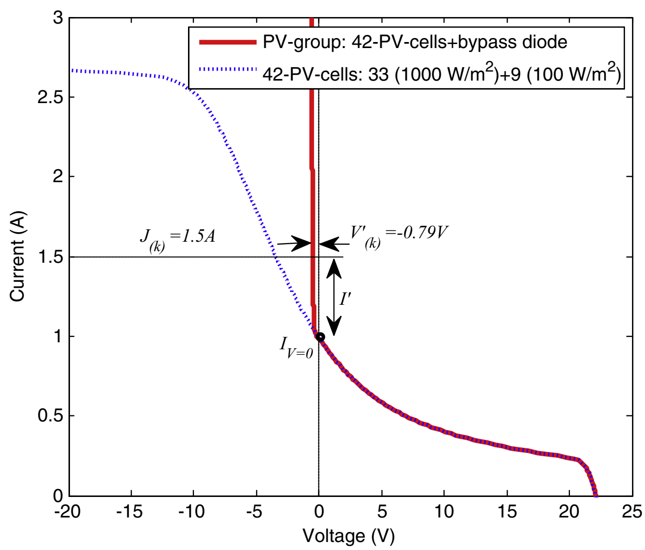

Fig. 8. Curves of PV-group.

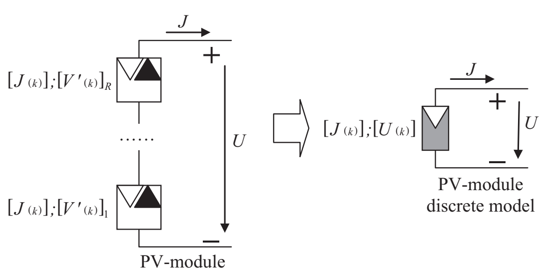

Fig. 9. Equivalent circuit of PV-module.

$$[J_{(k)}] = [J_{(1)}, J_{(2)}, \ldots, J_{(k)}, \ldots, J_{(K)}]$$
$$[U_{(k)}] = [U_{(1)}, U_{(2)}, \ldots, U_{(k)}, \ldots, U_{(K)}] \tag{24}$$

where

- $[U_{(k)}] = \sum_{r=1}^{R} \left[V'_{(k)}\right]_r$;
- $U_{(k)}$ is the PV-module voltage for current $J_{(k)}$.

As an example, the I–V curve for a shaded PV-module (see Fig. 10), formed by three PV-groups of 20 cells per group is shown in Fig. 11. The first PV-group has 4 fully shaded cells and 6 partially shaded (3 with 25% and 3 with 75% areas shaded); the second PV-group has 2 partially shaded cells (one with 25% and another with 75% shaded area) and, finally, the third represents an unshaded PV-group.

3.4. PV-string model

A PV-string is a series association of M PV-modules. Therefore, the following PV-module discrete vectors must be used:

$$\left[J_{(k)}\right]_{m=1,\ldots,M}; \left[U_{(k)}\right]_{m=1,\ldots,M} \tag{25}$$

where $[J_{(k)}] = [J_{(k)}]_1 = \cdots = [J_{(k)}]_m = \cdots = [J_{(k)}]_M$.

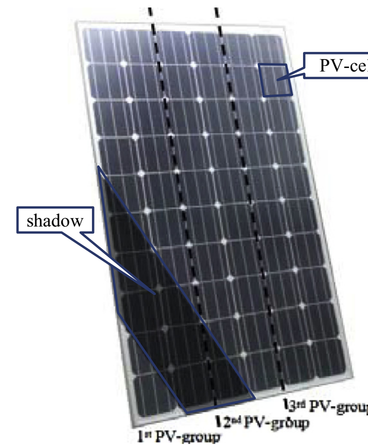

Fig. 10. Shaded PV-module of three PV-groups.

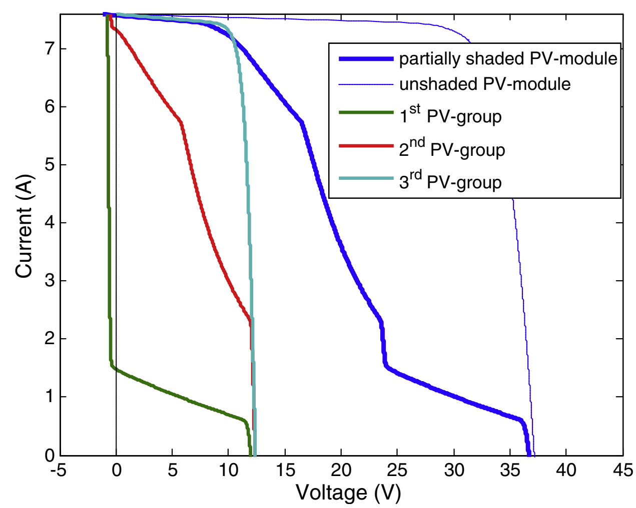

Fig. 11. Curve of shaded PV-module and its PV-groups.

In conclusion, the PV-string discrete model (see equivalent circuit of Fig. 12) can be defined by the vectors:

$$[J_{(k)}] = [J_{(1)}, J_{(2)}, \ldots, J_{(k)}, \ldots, J_{(K)}]$$
$$[U'_{(k)}] = [U'_{(1)}, U'_{(2)}, \ldots, U'_{(k)}, \ldots, U'_{(K)}] \tag{26}$$

where

- $U'_{(k)}$ is the PV-string voltage for current $J_{(k)}$;
- $[U'_{(k)}] = \sum_{r=1}^{M} [U_{(k)}]_r = \sum_{r=1}^{RxM} \left[V'_{(k)}\right]_r$.

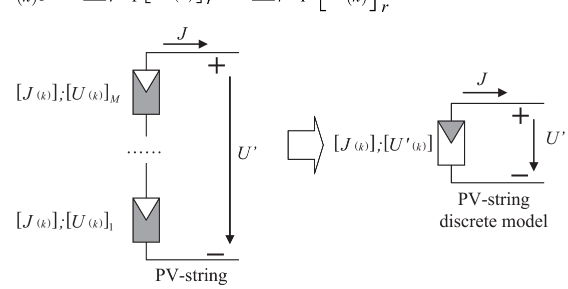

Fig. 12. Equivalent circuit of PV-string.

3.5. PV-array model

A PV-array is a parallel association of L PV-strings. Therefore, the PV-array discrete is formed by L PV-strings with the same voltage $U'_{(k)}$.

Parallel association has been analyzed using a similar technique than that shown in Section 3, taking into account that the common variable in this association is the voltage. As a consequence, the following discrete voltage vector is defined:

$$[U''_{(s)}] = [0, \Delta U, 2\cdot\Delta U, \ldots, s\cdot\Delta U, \ldots, S\cdot\Delta U] \tag{27}$$

where

- $U''_{(s)} = (s-1)\cdot\Delta U$;
- s is a positive integer number between $s = [1, \ldots, S]$ being S defined by $(S+1)\cdot\Delta U = NxRxM\cdot V_0$;
- V_0 is the open voltage of the PV-cell.

The corresponding discrete current vector $[J'_{(s)}]$ has to be obtained, where:

$$\left[J'_{(s)}\right] = \left[J'_{(1)}, J'_{(2)}, \ldots, J'_{(s)}, \ldots, J'_{(S)}\right] \tag{28}$$

It must be taken into account that the values for L current discrete vectors $\left[J_{(k)}\right]_1 \equiv \cdots \equiv \left[J_{(k)}\right]_L$ (see Fig. 13) and the corresponding L voltage vectors $\left[U'_{(k)}\right]_1$ to $\left[U'_{(k)}\right]_L$ are known.

To obtain $[J'_{(s)}]$, a linear interpolation technique can be used. The process is:

(1) For each element of defined voltage U'', the nearest values in the discrete vectors are obtained:

$$U''_{(s)} \rightarrow \begin{matrix} U'_{1(s_1-1)} < U''_{(s)} < U'_{1(s_1)} \rightarrow J_{1(s_1-1)}; J_{1(s_1)} \\ \cdots \\ U'_{L(s_P-1)} < U''_{(s)} < U'_{L(s_P)} \rightarrow J_{L(s_P-1)}; J_{L(s_P)} \end{matrix} \tag{29}$$

where s_r represents the index in the discrete vector $\left[U'_{(s)}\right]_r$ of the "r" PV-string for the nearest voltage to $U''_{(s)}$.

(2) Then, the linear interpolation is used:

$$\left.\begin{matrix} J'_{1(s)} = J_{1(s_1-1)} + \frac{\Delta I}{U'_{1(s_1)} - U'_{1(s_1-1)}}\cdot\left(U''_{(s)} - U'_{1(s_1-1)}\right) \\ \cdots \\ J'_{L(s)} = J_{L(s_P-1)} + \frac{+\Delta I}{U'_{L}(s_P) - U'_{L(s_P-1)}}\cdot\left(U''_{(s)} - U'_{L(s_P-1)}\right) \end{matrix}\right\} \tag{30}$$

(3) And, finally, each element of discrete vector of PV-array current $[J''_{(s)}]$ is:

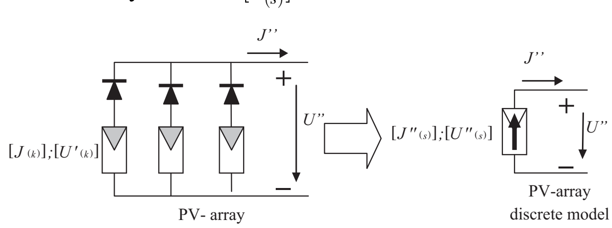

Fig. 13. Equivalent circuit of PV-array.

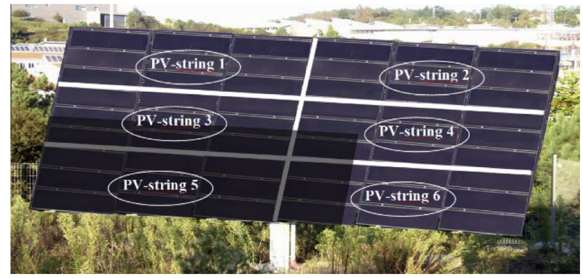

Fig. 14. PV-array on a tracker shaded by other tracker (UTM 29T 525820.68E 466832.28N).

$$J''_{(s)} = \sum_{i=1}^{P} J'_{i(s)} \tag{31}$$

As an example, a PV-array (see Fig. 14) formed by 6 PV-strings with 9 PV-modules each one has been analyzed. The system has been supposed under a beam irradiance G_b equals to 900 W/m^{2,} and a diffuse irradiance G_d equals to 100 W/m^2. In this situation, the following shading conditions has been studied:

- Unshaded: shading coefficients equals to one ($\sigma = 1$) in every cell.
- Partially shaded, with different shading coefficients ($\sigma = 0$–1) between cells. The shadow geometry for this case is shown in Fig. 14.
- Uniformly shaded, with a common shading coefficient equal to 0 ($\sigma = 0$).

As a result, the PV-array I–V curves shown in Fig. 15 have been obtained.

3.6. Application of discrete method to energy evaluation of PV-array

From the proposed discrete model can be obtained the electric power in PV-array by means of:

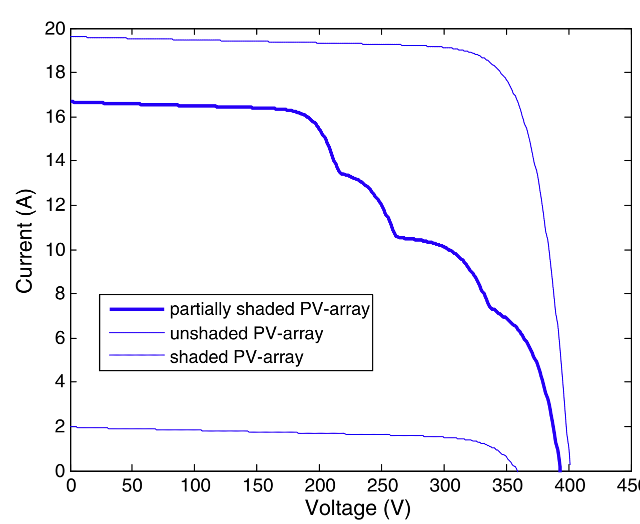

Fig. 15. Curve I–V of a shaded array.

$$[P_{(s)}] = [P_{(1)}, P_{(2)}, \ldots, P_{(s)}, \ldots, P_{(S)}] \quad (32)$$

where $P_{(s)} = U''_{(s)} \cdot J''_{(s)}$. From this equation, the Maximum Power Point (MPP) can be obtained using:

$$P^* = P_{(n)} = \max_n [P_{(1)}, P_{(2)}, \ldots, P_{(k)}, \ldots, P_{(S)}] \quad (33)$$

where "n" represents the index of $[P_{(s)}]$ for the MPP value P^*. Using the index "n" it is possible to obtain the voltage, current and power of any element of the PV system. This can be done by reverse searching of the indexes of discrete vectors that are involved in the calculation of the PV-array solution.

As an example, in Fig. 16 it is shown the power curve of the array of the example of Fig. 15. The Maximum Power Point (MPP) value is the maximum value of each power curve.

4. Examples and results

Within this section, several examples are presented to test the performance of the proposed discrete model. The first example is a PV-array formed by mono-crystalline modules with a shaded area that moves over time. The second one is a PV-array composed by CIS modules and with a shaded area that grows over time. Finally, the third one considers a PV-array with mono-crystalline modules, also with a shaded area that enlarges over time.

4.1. PV-array mono-crystalline with a shaded area that moves over time

This section analyses an array with 10 mono-crystalline modules disposed in one string of modules. Each module has three groups with 20 cells in each group (Fig. 17). A structural element causes a shadow of a rectangular shape. This shaded area changes with the sun's displacement. The width of this obstacle doubles the width of the cells. When the shadow is in the gap between modules 5 and 6 the PV-array is not shaded, and the power is at its maximum. Afterwards, the shadow moves itself and shades 5 modules.

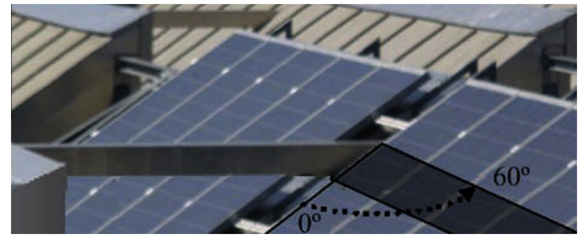

Fig. 17. PV-array shaded by a structural element.

In Fig. 18 it is shown the I–V characteristics for the installation of Fig. 17 considering the evolution of the shaded area from 0° to 60°. The power evolution is shown in Fig. 19 where the MPP values are represented by red circles.

4.2. PV-array CIS with a shaded area that grows over time

In this paragraph, an example of a tracker with 54 CIS modules disposed in 6 strings of 9 modules each one is considered. The arrangement of the modules is horizontal, and the modules of each string are disposed in columns (Fig. 20). In this example, the shaded area grows from 0% to 78% of the overall PV-array area.

The method proposed in II is used to calculate the I–V curves of rectangular shadows on the tracker (Fig. 21). The MPP of each curve has been obtained as shown in Fig. 22 (see red circles).

4.3. PV-array mono-crystalline with a shaded area that grows over time

In this case, an example of a tracker with 2 strings of 10 modules in series association is studied. Each module is formed by 3 groups of 24 cells with a serial bypass diode

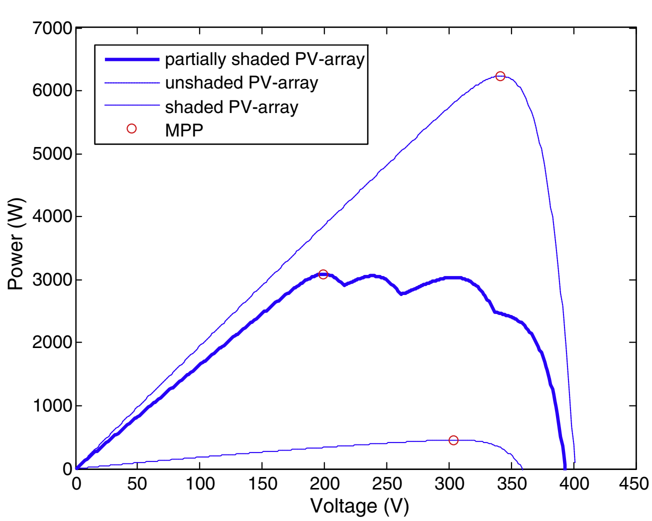

Fig. 16. Curve P–V of an array.

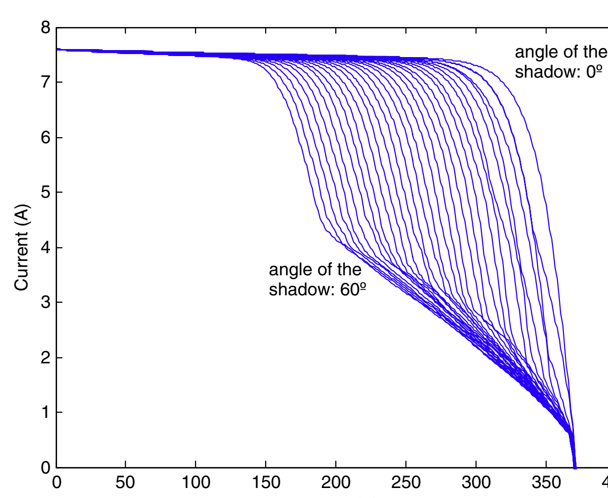

Fig. 18. I–V curves of an array with shadows of a structural element.

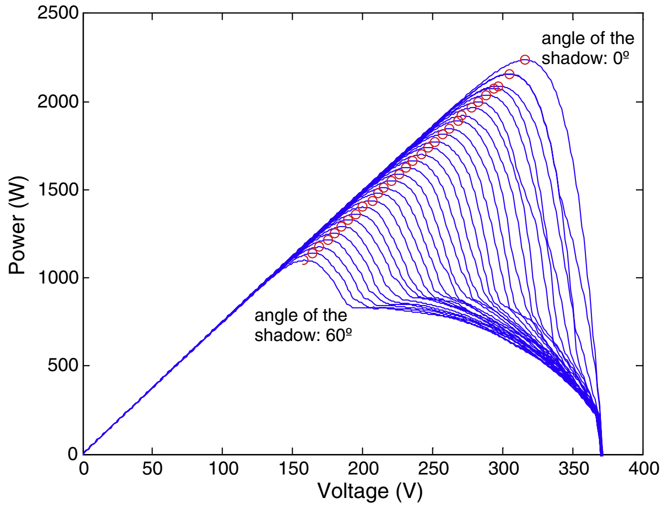

Fig. 19. *P–V* curves of an array with shadows of a structural element.

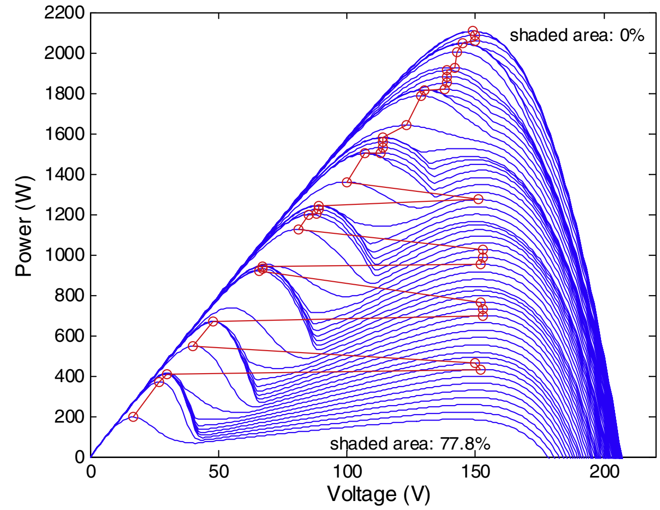

Fig. 22. *P–V* curves of a PV-array with shadows.

Fig. 20. PV-array with 6 strings of 9 CIS modules each one(UTM 29T 525820.68E 466832.28N).

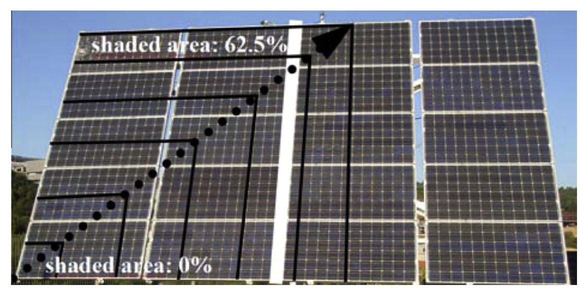

Fig. 23. PV-array with 2 strings of 10 mono-crystalline modules each one(UTM 29T 525820.68E 466832.28N).

on each one. The arrangement of the modules is horizontal, and the modules of each string are disposed in two columns (Fig. 23).

The results obtained with the proposed method are shown in Fig. 24 and Fig. 25, when a rectangular shadow grows as presented in Fig. 23 (from 0% to 62.5% of the area).

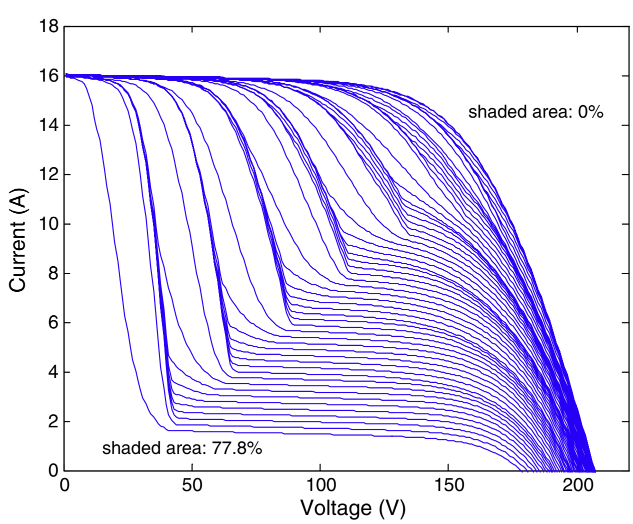

Fig. 21. *I–V* curves of an array with shadows.

5. Conclusions

This paper presents a simple and fast method for calculating the *I–V* curve of partially shaded PV installations. Nevertheless, the method can be used for any irradiance and temperature conditions in PV-cells.

The method is based on the discretization of currents and voltages in the PV-cells and in the bypass diode. The relation between current and voltage in PV-cells is established using a non-linear implicit function where the irradiance and temperature are considered. These implicit functions are solved by using a Newton–Raphson algorithm.

The partial shading in the PV-cell is modelled by different irradiance levels between cells.

The proposed method allows the modelling of a PV-array by a pair of vectors of current and voltage. Accordingly, the *I–V* characteristic of the PV-array can be obtained by discrete modelling. Through this modelling, any electrical variable, e.g. power or energy, can be easily calculated.

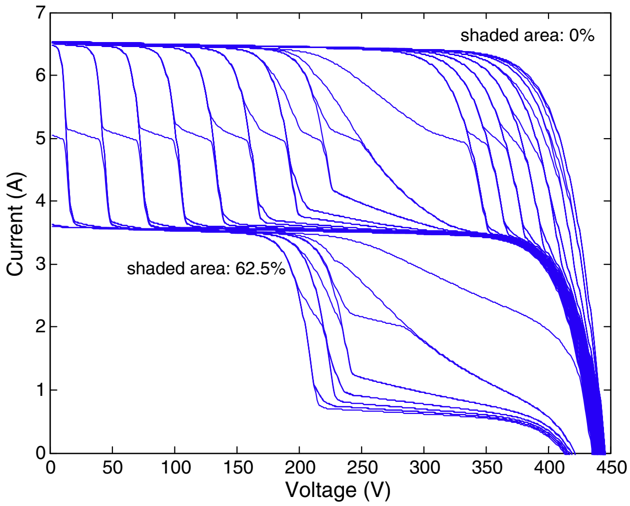

Fig. 24. *I–V* curves of a PV-array with the shadows of Fig. 23.

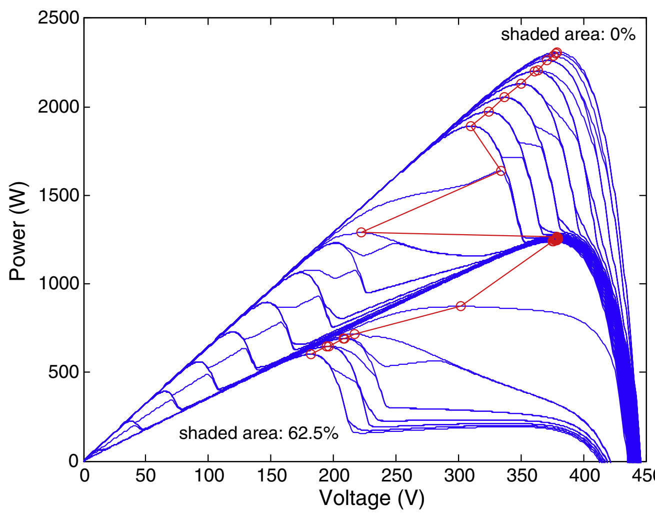

Fig. 25. *P–V* curves of a PV-array with the shadows of Fig. 23.

Since the irradiance and temperature for every single PV-cell is taken into account, the proposed model for the PV-array can be used to analyze any shading and temperature condition (variable shadows, irregular shadows, hot spots, etc.).

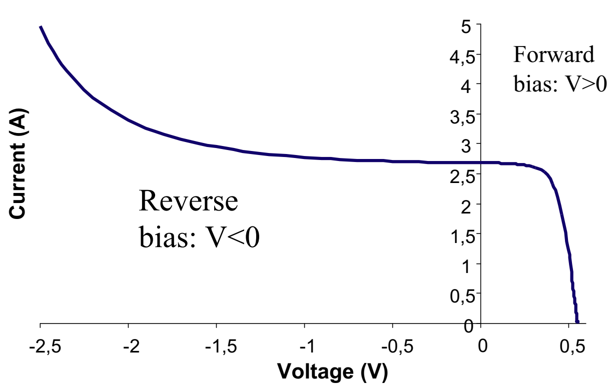

Fig. 26. *I–V* curves of forward and reverse bias of a CIS cell.

Moreover, the proposed modelling allows for the calculating of every electrical variable in any PV-cluster (PV-cells, PV-module…).

The paper finally concludes with three examples of PV-arrays under different shading conditions where the simplicity, capacity and flexibility of the proposed discrete model are demonstrated.

Acknowledgments

This work was supported in part by the Consellería of Innovación e Industria (Xunta de Galicia, Spain) under contract 07REM008V19PR and the Ministry of Science and Innovation (Spain) under contract ENE 2009-13074.

Appendix A

CIS PV-cell behaviour

Fig. 26 shows the curve for forward and reverse biasing of a PV-cell which has been obtained experimentally with an irradiance of 1000 W/m^2 (Braunger et al., 1996; Szaniawski et al., 2013;).

Crystalline PV-cell behaviour

The curves of crystalline PV-cells were obtained under conditions of complete darkness using a current source. It has been found out that the *I–V* curves have a large scattering in the inverse bias region (Alonso-García and Ruíz, 2006; Bauer et al., 2009).

PV-cell parameters

Appendix B

The set of equations for a PV-group is:

$$\begin{cases} \text{N-PV-cells in series } [f(V_i, I, G_i)] = [0] \\ \text{Bypass diode in parallel } \; I' = I_0 \cdot (e^{\frac{-qV}{k_B T}} - 1) \\ V = \sum_{i=1}^{N} V_i \\ J = I + I' \end{cases} \tag{34}$$

When the voltage in the diode is around its forward voltage ($V_0 = -0.7$ V), then the PV-group can be modelled by means the following equations (see Fig. 27):

$$I = I_{(V_0)} + \Delta I \approx I_{(V_0)} - \frac{1}{\rho} \cdot \Delta V \tag{35}$$

$$I' \approx I'_{d0} + \Delta I' \approx \Delta I' = -\frac{1}{\rho'} \cdot \Delta V \tag{36}$$

where

- I' *is* the current the bypass diode current for forward bias.
- $I = I_{(V0)} + \Delta I$ is the current in N-PV-cells.
- ρ is the equivalent resistance of N-PV-cells and it is defined by (35) using the values of the vector (15).
- ρ' is the equivalent resistance of bypass diode, and it is defined by (36).

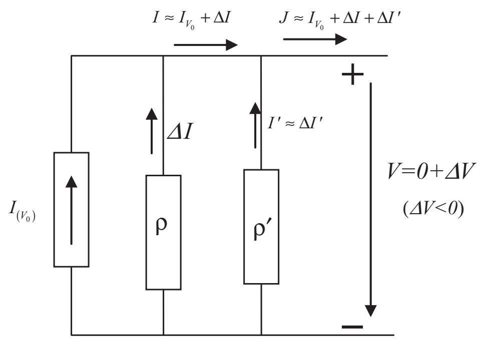

Fig. 27. Linear circuit of PV-group.

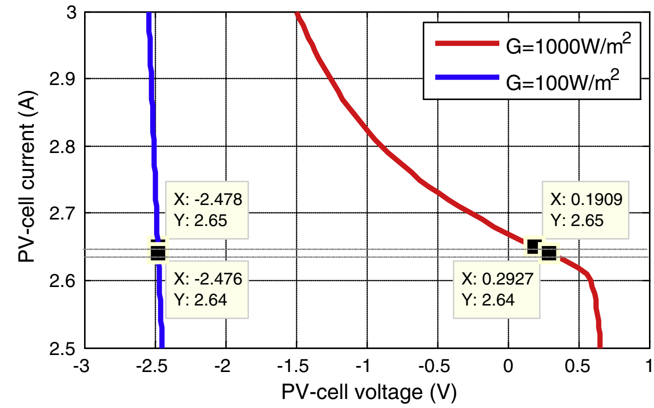

Fig. 28. I–V curves of PV-cell values at different irradiance levels.

Using those equations the following relations can be established:

$$\left.\begin{array}{l} \Delta V = \sum_{i=1}^{N}\Delta V_i = \sum_{i=1}^{N}\left.\frac{dV_i}{dI}\right|_{V_0}\cdot\Delta I \equiv -\left(\sum_{i=1}^{N}\rho_i\right)\cdot\Delta I \equiv -\rho\cdot\Delta I \\ \Delta V = \left.\frac{dV}{dI'}\right|_{V_0}\cdot\Delta I' \equiv -\rho'\cdot\Delta I' \\ \left.\frac{dV_i}{dI}\right|_{V_0} \approx \left.\frac{\Delta V_i}{\Delta I}\right|_{V_0} \\ \frac{dV}{dI'} = \frac{k_B T}{q}\left(\frac{1}{I'_{V_0}+I_0}\right) = \rho' \end{array}\right\}$$

$$\rightarrow \begin{array}{l} \Delta I = \frac{\rho'}{\rho+\rho'}\cdot\Delta J \\ \Delta I' = \frac{\rho}{\rho+\rho'}\cdot\Delta J \end{array} \qquad (37)$$

where for $V = 0$ results $\rho \ll \rho' \approx 5000\ \mathrm{M\Omega}$ and consequently:

$$\left.\begin{array}{l} \Delta I \approx \Delta J \\ \Delta I' \approx 0 \end{array}\right\} \rightarrow J \approx I_{V=0} + \Delta I \qquad (38)$$

And, for $V < V_0$ results $\rho \gg \rho' \approx 0.008\ \Omega$ so:

$$\left.\begin{array}{l} \Delta I \approx 0 \\ \Delta I' \approx \Delta J \end{array}\right\} \rightarrow J \approx I_{V_0} + \Delta I' \approx I_{V=0} + \Delta I' \qquad (39)$$

As an example, it is analyzed a PV-group when its total voltage is around zero ($V \approx 0$). It is supposed to be composed by 10 CIS PV-cells with 9 of them with an irradiance of 1000 W/m^2 and the last one with 100 W/m^2 (diffuse irradiance). The resulting I–V curves for the different PV-cells are shown in Fig. 28. In this situation, the elements i and $i+1$ in discrete vectors are shown in Table 2, where:

- u is the voltage of each PV-cell with $G = 1000$ W/m^2;
- v is the voltage of PV-cell with $G = 100$ W/m^2;
- V is the voltage of PV-group: $V = 9\cdot u + 1\cdot v$.

So, the equivalent resistance is determined by:

$$\rho = -\left((N-H\cdot)\frac{\Delta u}{\Delta I} - H\cdot\frac{\Delta v}{\Delta I}\right)$$
$$= -\left(9\cdot\frac{0.1909-0.2927}{0.01} - 1\cdot\frac{2.4777-2.4757}{0.01}\right)$$
$$= 91.42\ \Omega$$

Table 1
Parameters of PV-cells.

	Crystalline	CIS
I_0 (A/cm^2)	$5.5\cdot 10^{-9}$	$9.3\cdot 10^{-10}$
I_{L0} (A/cm^2)	$32.7\cdot 10^{-3}$	$26.8\cdot 10^{-3}$
R_s (Ω cm^2)	0.5	3.5
R_p (Ω cm^2)	1000	1200
n	1.5	1.25
V_{br} (V)	−15	−4
m	3.8	3.8
α	0.35	0.35
s (cm^2)	10 × 10	125 × 0.8

Table 2
Resulting i and $i+1$ elements of discrete vectors.

	V	I	u	v
i	0.1586	2.64	0.2927	−2.4757
$i+1$	−0.7596	2.65	0.1909	−2.4777

And the PV-cell current for $V = 0$ and $V = -0.7$ V can be determinated by the numerical linear interpolation:

$$I_{V=0} \approx I(i) + \frac{\Delta I}{V(i+1)-V(i)}(0 - V(i)) = 2.64 + \frac{0.1586}{\rho}$$
$$= 2.6417\ \mathrm{A}\, I_{V=-0.7}$$
$$\approx I(i) + \frac{\Delta I}{V(i+1)-V(i)}(-0.7 - V(i))$$
$$= 2.64 + \frac{0.8586}{\rho} = 2.6494\ \mathrm{A}$$

Appendix C

Discretization step for current
The derivate of the implicit function (1) is:

$$df = \frac{\partial f}{\partial V}\cdot dV + \frac{\partial f}{\partial I}\cdot dI = 0 \rightarrow \frac{dV}{dI}$$
$$= -\left(\frac{\partial f}{\partial I}\right)\cdot\left(\frac{\partial f}{\partial V}\right)^{-1} \qquad (40)$$

where

$$\left(\frac{\partial f}{\partial V}\right) = I_0 \frac{q}{k_B T} e^{\frac{q(V+IR_s)}{k_B T}} + \frac{1}{R_p} + \frac{1}{R_p}\alpha\left(1 - \frac{V+IR_s}{V_{br}}\right)^{-m} + \frac{V+IR_s}{R_p}\alpha m\left(1 - \frac{V+IR_s}{V_{br}}\right)^{-m-1}\frac{1}{V_{br}}\left(\frac{\partial f}{\partial I}\right) = 1 + R_s\left(\frac{\partial f}{\partial V}\right)$$

For a given discretization step Δu, the minimum discretization step ΔI, when u is around zero, and using (40) is:

$$\Delta I < \Delta u\left(\frac{\partial f}{\partial I}\right)\bigg|_{V=0}\left(\left(\frac{\partial f}{\partial V}\right)\bigg|_{V=0}\right)^{-1} \quad (41)$$

Thus, using the parameters in Table 1, this value for a CIS cell is $\Delta I < \Delta u/9.4$ and, for a crystalline cell is $\Delta I < \Delta u/7.5$.

References

Alonso-García, M.C., Ruíz, J.M., 2006. Analysis and modelling the inverse characteristic of photovoltaic cells. Sol. Energy Mater. Sol. Cells 90, 1105–1120.

Alonso-García, M.C., Ruíz, J.M., Herrmann, W., 2006. Computer simulation of shading effects in photovoltaic arrays. Renew. Energy 31, 1986–1993.

Alonso-García, M.C. et al., 2006a. Experimental study of mismatch and shading effects in the I–V characteristic of a photovoltaic module. Sol. Energy Mater. Sol. Cells 90, 329–340.

Bauer, J., Wagner, J.-M., Lotnyk, A., Blumtritt, H., Lim, B., Schmidt, J., Breitenstein, O., 2009. Hot spots in multicrystalline silicon solar cells: avalanche breakdown due to etch pits. Phys. Status Solidi RRL 3 (2–3), 40–42.

Bishop, J.W., 1988. Computer simulation of the effects of electrical mismatches in photovoltaic cell interconnection circuits. Sol. Cells 25, 73–89.

Braunger, D., Hariskos, D., Walter, T., Schock, H.W., 1996. An 11. 4% efficient polycrystalline thin film solar cell based on CuInS2 with a Cd-free buffer layer. Sol. Energy Mater. Sol. Cells 40, 97–102.

Caluianu, I., Notton, G., Colda, I., Caluianu, S., Damian, A., 2009. Photovoltaic energy generation under partially shading conditions. In: Electromotion 2009 – EPE Chapter 'Electric Drives' Joint Symposium.

Chatterjee, A., Keyhani, A., Kapoor, D., 2011. Identification of photovoltaic source models. IEEE Trans. Energy Convers. 26, 883–889.

Chen, Shuanghong et al., 2010. Numerical model analysis of the shaded dye-sensitized solar cell module. J. Phys. D: Appl. Phys. 43, 305102 (6 pp).

Di Piazza, M.C., Vitale, G., 2010. Photovoltaic field emulation including dynamic and partial shadow conditions. Appl. Energy 87, 814–823.

Díaz-Dorado, E., Suárez-García, A., Carrillo, C., Cidrás, J., 2010. Influence of the shadows in photovoltaic systems with different configurations of bypass diodes. In: 20th International Symposium on Power Electronics, Electric Drives, Automation and Motion.

Díaz-Dorado, E., Suárez-García, A., Carrillo, C., Cidrás, J., 2010. Influence of the PV modules layout in the power losses of a PV array with shadows. In: EPE-PEMC 2010. 14th International Power Electronics and Motion Control Conference.

Díaz-Dorado, E., Suárez-García, A., Carrillo, C.J., Cidrás, J., 2011. Optimal distribution for photovoltaic solar trackers to minimize power losses caused by shadows. Renew. Energy 36, 1826–1835.

García, M., Maruri, J.M., Marroyo, L., Lorenzo, E., Pérez, M., Shadowing, "Partial, 2008. MPPT performance and inverter configurations: observations at tracking PV plants. Prog. Photovolt.: Res. Appl. 16, 529–536.

Gordon, J.M., Wenger, H.J., 1991. Central-station solar photovoltaic systems: field layout, tracker, and array geometry sensitivity studies. Sol. Energy 46, 211–217.

Karatepe, E., Boztepe, M., Çolak, M., 2006. Development of a suitable model for characterizing photovoltaic arrays with shaded solar cells. Sol. Energy 81, 977–992.

Kawamura, H. et al., 2003. Simulation of I–V characteristics of a PV module with shaded PV cells. Sol. Energy Mater. Sol. Cells 75, 613–621.

Martínez-Moreno, F., Muñoz, J., Lorenzo, E., 2010. Experimental model to estimate shading losses on PV arrays. Sol. Energy Mater. Sol. Cells 94, 2298–2303.

Narvarte, L., Lorenzo, E., 2008. Tracking and ground cover ratio. Progr. Photovolt. Res. Appl. 16 (2008), 703–714.

Perpiñán, O., 2012. Cost of energy and mutual shadows in a two-axis tracking PV system. Renew. Energy 43, 331–342.

Petrone, G., Ramos-Paja, C.A., 2011. Modeling of photovoltaic fields in mismatched conditions for energy yield evaluations. Electr. Power Syst. Res. 81, 1003–1013.

Petrone, G., Spagnuolo, G., Vitelli, M., 2007. Analytical model of mismatched photovoltaic fields by means of Lambert W-function. Sol. Energy Mater. Sol. Cells 91, 1652–1657.

Quaschning, V., Hanitsch, R., 1996. Numerical simulation of current–voltage characteristics of photovoltaic systems with shaded solar cells. Sol. Energy 56, 513–520.

Silvestre, S., Chouder, A., 2008. Effects of shadowing on photovoltaic module performance. Prog. Photovolt.: Res. Appl. 16, 141–149.

Silvestre, S., Bornat, A., Chouder, A., 2009. Study of bypass diodes configuration on PV modules. Appl. Energy 86, 1632–1640.

Szaniawski, P., Lindahl, J., Törndahl, T., Zimmermann, U., Edoff, M., 2013. Light-enhanced reverse breakdown in Cu(In, Ga)Se2 solar cells. Thin Solid Films 535, 326–330.

Wang, Y.J., Hsu, P.C., 2011. Modelling of solar cells and modules using piecewise linear parallel branches. IET Renew. Power Gener 5 (3), 215–222.

Woyte, A., Nijs, J., Belmans, R., 2003. Partial shadowing of photovoltaic arrays with different system configurations: literature review and field test results. Sol. Energy 74, 217–233.